Comparison of the Dynamic Response of Radial and Tangential Magnetic Flux Thrust Bearings

Andrew Kenny and Alan B. Palazzolo

***Abstract*—Theoretical predictions were made for the dynamic performance of a tangential flux magnetic thrust bearing. A prototype bearing was built with the stators and rotors made from tape wound strip. The performance of this bearing was measured and compared to the theoretical predictions and also to the performance of a radial flux thrust bearing. Tangential flux bearings are intrinsically amenable to construction from tape wound cores. Tape wound cores come in high saturation alloys like supermenduer which can give the bearing a high force to size ratio. The thin tape laminates give the bearing a broad frequency bandwidth. By comparison it is shown that it is difficult to make a laminated rotor magnetically efficient for radial flux bearings. A test rig is described that was built to measure the performance of the tangential flux bearing. A power amplifier with current feedback provided dc and harmonic current to the coils. A load cell was built into the test rig to measure the axial thrust, an inductive/hall sensor was included to measure the coil current, and a hall probe to measure the gap flux.**

***Index Terms*—Magnetic bearing, magnetic circuit, tape wound core.**

NOMENCLATURE

A	Half pole face area.
d	Laminate thickness or thinnest dimension of flux path.
D_i	Denominator terms.
f	Stacking factor.
F	Magnetic force per stator.
Φ	Magnetic flux.
I_c	Coil current.
l	Path length.
L	Coil inductance.
L_i	Inductive parts of laminate reluctance.
n_p	Number of poles per stator.
N_i	Numerator terms.
$(NI)_b$	Turns per coil times bias current.
$(NI)_c$	Turns per coil times control current.
μ	Permeability of metal.
μ_0	Permeability of air.
$\mu_{\rm rel}$	Relative permeability of metal
$\mu_{\rm stackn}$	Permeability normal to laminations.
$\mu_{\rm stackt}$	Permeability tangential to laminations.
$\rho_{\rm lam}$	Density of laminate metal.
ρ_a	Density of laminate adhesive.
R_i	Resistive parts of reluctance.
R_s	Stator reluctance of circuit.
R_r	Rotor reluctance of circuit.
R_{dc}	$0-$ Hz reluctance of path.
R_b	Bias reluctance.
R_c	Control reluctance.
s	Complex frequency.
ω	Magnetic circuit frequency.

Manuscript received October 26, 2000; revised August 17, 2001. Recommended by Technical Editor B. Ravani. This work was supported in part by the U.S. Navy under Grant ONR BAA97-030.

The authors are with the Texas A&M University, College Station, TX 77843 USA (e-mail: a-kenny@ tamu.edu; a-palazzolo@ tamu.edu).

Publisher Item Identifier S 1083-4435(02)01673-3.

I. INTRODUCTION

MOST MAGNETIC thrust bearings are the radial flux path type. This bearing has an annular electromagnet stator which attracts a disk on the rotor [1]. The magnetic flux travels in the radial direction as it circles the electromagnet coil. A laminated rotor increases this type of bearing's magnetic path dc reluctance so the rotor is usually a solid disk. Thus the main draw back of this type of bearing is its low frequency response caused by induced eddy currents.

The tangential flux path type of thrust bearing described in this paper has an even number of coils through which the flux travels tangential to the bearing circumference. This is similar to, but different than the type of tangential flux thrust bearing that uses separate C cores [2], [3]. The flux travels tangential to the laminations when the rotor and stator are made from circular tape wound strip. The laminations reduce eddy currents and give this type of bearing a high frequency response. The major disadvantage of this type of bearing is its low rotor revolution speed that is limited by the strength of the rotating tape wound disk.

II. TANGENTIAL FLUX THRUST BEARING

A tangential flux thrust bearing has a toroid thrust runner disk with a stator on each side. The stators are also toroids, but with slots cut to form poles and give space for the coil windings. Fig. 1 shows the geometry of the assembly.

Both the runner and stator toroids can be made from tape-wound strip. The strips are adhesively bonded together to make the toroids solid laminated cores.

As shown by the flux arrows and coil current direction arrows on Fig. 2, the polarity of the coils is important to obtain the correct magnetic flux paths. The flux that exits one stator pole reenters the stator through the two adjacent poles. The path that connects the stator poles is in the rotor. The rotor cross section area must equal the pole cross section area. A bearing with a four pole bearing will require a runner that is twice as thick as a bearing with an eight pole stator.

The polarity of the poles in the top and bottom stator is arranged so that the flux from the top stator repels the flux from

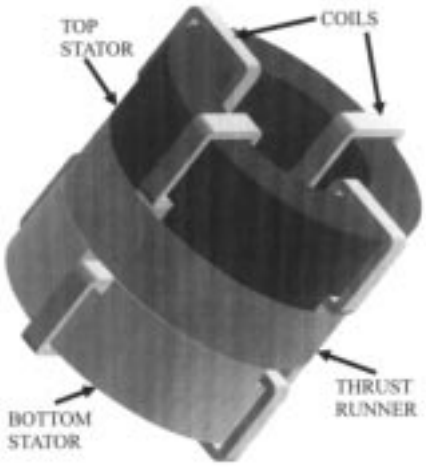

Fig. 1. Geometry of the rotor and stator in a tangential flux thrust bearing.

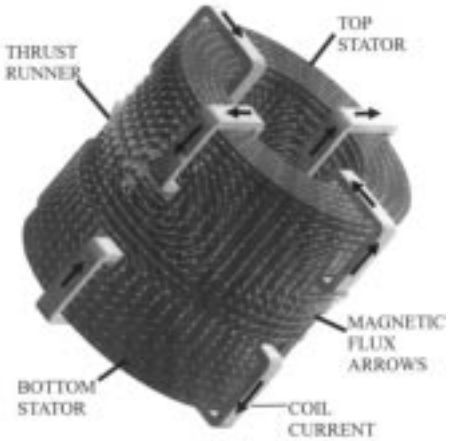

Fig. 2. Flux path and pole polarity in a tangential flux thrust bearing.

the bottom stator. The time-varying control flux is superposed on the bias flux by superposing a control current on the bias current in each coil. In the stators both the bias flux and control flux follow the same path. In the rotor the bias flux from the top stator occupies the rotor top half and the bias flux from the bottom stator flows in the rotor bottom half. The control flux from the top and bottom stators uses the entire thickness of the rotor.

The control current is simultaneously added to the coils in the top stator as it is subtracted from the coils in the bottom stator. The magnetic force between the stator and the rotor is given by (1) [4]. The force is directly proportional to the control current

$$F = \frac{(NI)_b\,(NI)_c\,A \cdot 2n_p}{\mu_0}. \tag{1}$$

The analytical method reported by Kucera and Ahrens [5] and advanced by Meeker, Maslen, and Noh [6] was one method used to study the time harmonic frequency response of the magnetic flux. It is based on an equation that predicts the decrease in magnitude and phase of the permeability for an increase in the frequency of the magnetic flux. The form derived theoretically from Maxwell's equations is given by (2) [7]. The method presented here is an alternative approach to modeling the magnetic

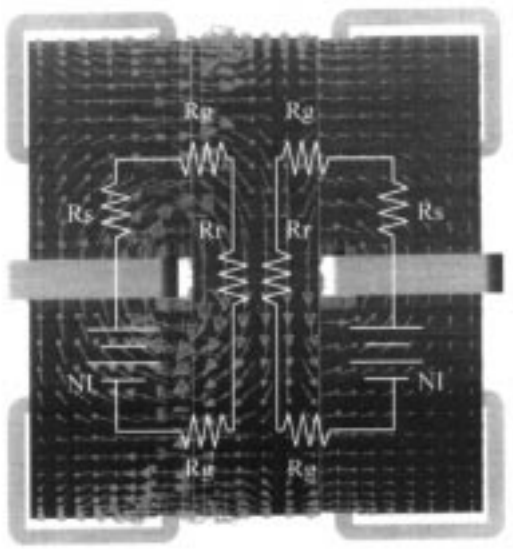

Fig. 3. Fundamental magnetic circuit path in the tangential flux bearing.

control force with a first order time lag as presented by Fukata, Kouya, *et al.* [8]

$$\mu = \mu_{\rm rel}\mu_0 \frac{\tanh\gamma}{\gamma} \tag{2}$$

where

$$\gamma = d\sqrt{j\omega\mu\sigma}. \tag{3}$$

The frequency dependent permeability is used in the calculation of the magnetic circuit path reluctance. Fig. 3 shows the fundamental magnetic circuit for two coils. This circuit flux path goes through two poles, two air gaps and the rotor. In a bearing with a four pole stator, there are four identical circuits of this type per stator. The reluctance of the stator and rotor sections increases with frequency according to (4) since the permeability decreases with frequency. The magnetic flux through the loop, is given by (5). The control force is directly proportional to the control flux, as in (1), so increasing the frequency decreases the force

$$R = \frac{l}{\mu A} \tag{4}$$

$$\Phi = \frac{(NI)_c}{R_s + R_r + 2R_g}. \tag{5}$$

Meeker, Maslen, and Noh showed that the hyperbolic tangent function in (2) can be replaced by a series and so the reluctance of any element in the circuit can also. The first three terms in the series are given for example in (6). As the thickness decreases, the resistance terms, calculated in (8), increases. Thus thin laminates do not see a decrease in permeability until high frequencies are reached

$$R_{\rm rotor} = R_{dc} + \cfrac{s}{R_1 + \cfrac{1}{sL_1} + \cfrac{1}{R_2 + \cfrac{1}{\cfrac{1}{sL_2} + \cfrac{1}{R_3 + \cfrac{1}{sL_3}}}}} \tag{6}$$

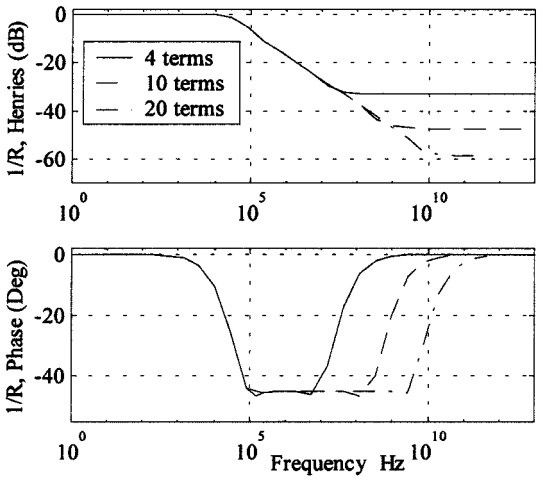

Fig. 4. Reciprocal of laminated path reluctance.

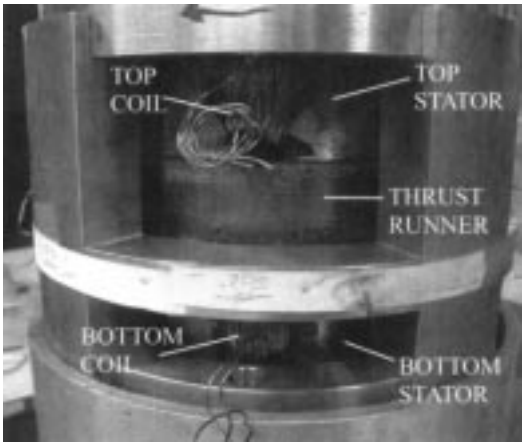

Fig. 5. Photograph of tangential flux bearing in the test rig.

where

$$L_i = \frac{\mu_0 \mu_r A}{(4 \cdot i + 1) l} \tag{7}$$

$$R_i = \frac{4(4 \cdot i - 1) A}{\sigma \cdot L_i \cdot d^2}. \tag{8}$$

Any needed number of terms can be added to (6) using a program loop in the Matlab [9] symbolic toolbox and then the series can be converted to an expression with a single numerator and denominator like (9)

$$R = \frac{N_0 + N_1 s + N_2 s^2 + N_3 s^3 + \cdots}{D_0 + D_1 s + D_2 s^2 + D_3 s^3 + \cdots}. \tag{9}$$

As the needed number of terms in (6) is increased, the frequency range over which the linear approximation is accurate is increased. This can be seen in Fig. 4 which shows the reciprocal of the reluctance of the laminated path for the four, ten, and twenty term approximations.

To obtain the frequency response of the flux, the reluctance of the two air gaps must be added to the frequency dependent laminated path reluctance. The inverse of this total reluctance has the frequency response of the flux, as given by (5). This is directly related to the frequency response of the bearing force.

The frequency response shown in Fig. 4 is what was predicted for the tape wound sections in our prototype tangantial flux bearing. It had four poles, a thrust runner I.D. of 5.08 cm (2.00 in), an O.D. of 12.98 cm (5.109 in), and thickness of 3.302 cm (1.300 in). The area of each of the poles was 111.4 cm^2 (17.26 in^2). Each coil had 80 turns. Both the runner and the stators were tape wound cores of 50 micron (2 mil) thick non grain oriented six percent silicon iron. The conductivity and relative permeability used for the silicon iron were $2 \cdot 10^6$/ohm m and 5000. The surfaces of the rotor and the pole surfaces were ground smooth to insure an even .43 mm (.017 in) gap under all the poles. After grinding the surfaces were etched to prevent interlaminate shorting. A photograph of the bearing in our test rig is shown in Fig. 5. Cross section views of the bearing in the test rig are shown through the poles and through the coils in Fig. 6.

The thrust runner is clamped between two plates to the shaft which is supported by linear bearings. The shaft axial motion is restrained by connection to a load cell at the bottom of the test rig. Low frequency force measurements can be made with this set up, but high frequency measurements not only measure the magnet force on the runner, but also the inertial force. Therefor high frequency measurements were limited to flux density readings in the gap. Shims were pushed in the top and bottom gaps to maintain the .43 mm (.017 in) distance during the high frequency testing. Since the force is known to be directly dependent on the flux density, this provided an indirect measurement of the force at high frequencies.

For completeness a three dimensional linear time harmonic finite element analysis was made on a model of a single laminate in the tape wound rotor and stator. It employed the symmetry of the four pole stator as shown in Fig. 7 to improve calculation efficiency. Just a single laminate was modeled in order to account for the thickness effect on the eddy currents.

The comparison of the gap flux magnitude versus frequency as determined by the circuit model, the finite element model and the test rig measurements is shown in Fig. 8. The circuit model and finite element model predictions are in good agreement up to the three decibel cutoff frequency of the bearing.

The flat bandwidth of the power electronics controlling the coil current in our test rig was limited to 2000 Hz, which is the reason the experimental data only goes up to this frequency. The power amplifier had a switching frequency of 22 kHz, which is one reason for the limited bandwidth of the power electronics. Another is that the inductance of each coil in the bearing was 4.18 mH and to produce 0.1 T in the air gap required 1.2 A per coil at 0 Hz. As (10) indicates, a supply of over 63 000 volts would be required to maintain this current at the predicted 3 dB frequency of nearly 2 MHz

$$V = I_c L \omega. \tag{10}$$

This is why we found it necessary to use the theoretical predictions as well as measurements to characterize the performance of the tangential flux thrust bearing.

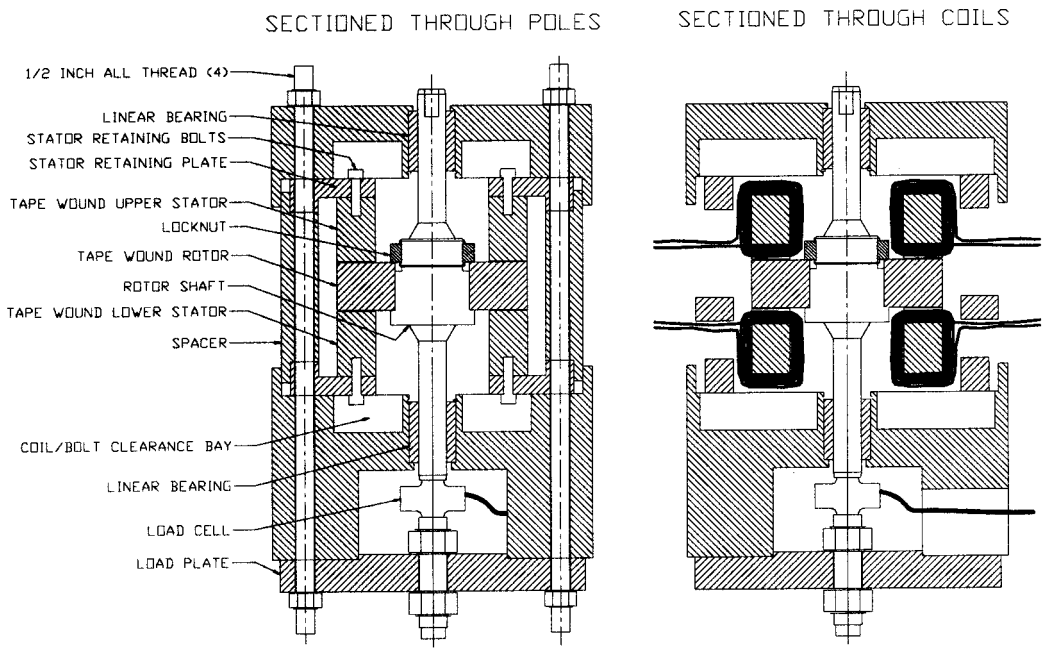

Fig. 6. Cross sections of bearing in test rig.

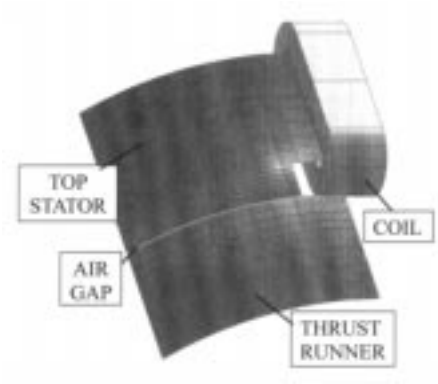

Fig. 7. Single laminate three-dimensional finite element analysis model employing symmetry of tangential flux thrust bearing. It shows current density contours at 5 MHz.

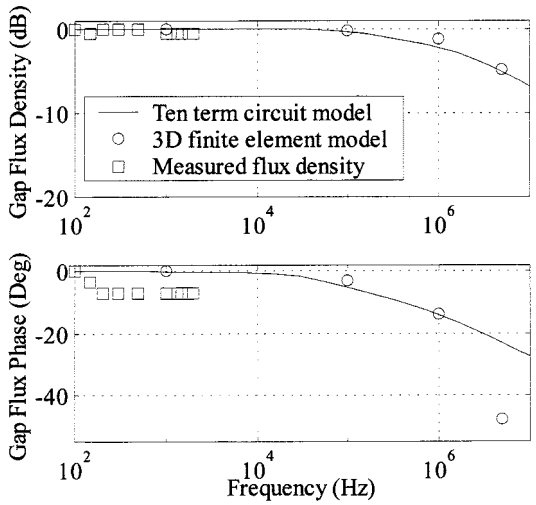

Fig. 8. Comparison of prediction and measurements on tangential flux thrust bearing.

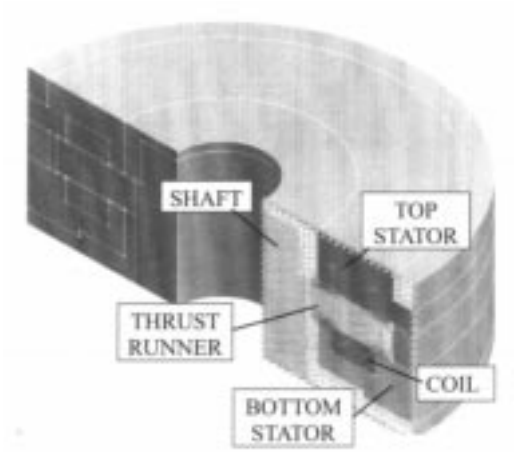

Fig. 9. Radial flux thrust bearing.

III. Radial Flux Thrust Bearing

A radial flux thrust bearing has a coil tangent to the rotor circumference. This coil lies in a slot in the stator. The walls of the stator slot may be made from circular tape wound laminations. The bottom of the slot can be a stack of flat laminates. Fig. 9 shows a two dimensional axisymmetric finite element model of the radial flux thrust bearing on which measurements were made for this study.

If the rotor is made from a flat stack of laminates the flux path enters the rotor normal to the stack. The rotor is usually made of a solid unlaminated disk partly because the anisotropic permeability of laminated structures requires they be oriented so that the flux path is tangent to the laminations. This was shown by Barton [10] by (11) and (12)

$$\mu_{\text{stackt}} = \mu_{\text{rel}}(1-f)+f \tag{11}$$

$$\mu_{\text{stackn}} = \frac{\mu_{\text{rel}}}{\mu_{\text{rel}}(1-f)+1}. \tag{12}$$

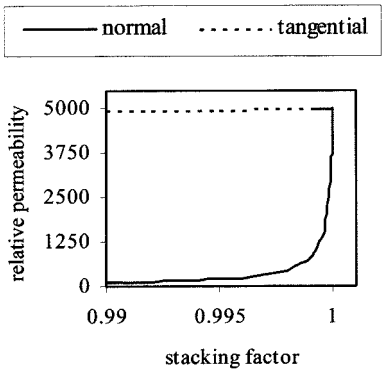

Fig. 10. Dependence of relative permeability on stacking factor.

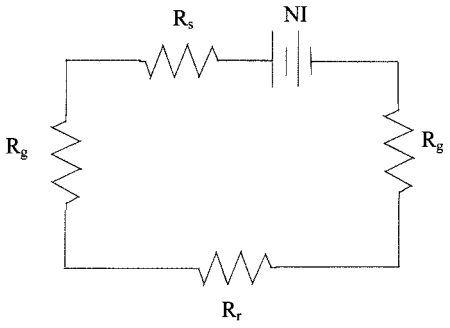

Fig. 11. Magnetic circuit for radial flux thrust bearing.

These equations give the dependence of the relative permeability normal and tangential to the stack as a function of the stacking factor. This dependence is plotted in Fig. 10. We made measurements on two stacks of rotor laminates made from 17.8 mm (0.7 in) and 8.8 mm (0.35 in) thick stacks of 0.15 mm (0.006 in) thick adhesive bonded laminates with a diameter of 44.5 mm (1.75 in). From (14), they were determined to have stacking factors of 0.981 and 0.987

$$f = \frac{\text{mass}_{\text{stack}} - \rho_a \cdot \text{volume}_{\text{stack}}}{(\rho_{\text{lam}} - \rho_a) \cdot \text{volume}_{\text{stack}}}. \tag{13}$$

In a radial flux thrust bearing the eddy currents naturally travel tangential to the circumference [11]. They also travel tangential to the laminations in a stacked rotor. Thus the laminations are ineffective. By contrast the eddy currents would try to flow normal to the tape wound laminates in the tangential flux thrust bearing. This is true for both the time-varying flux induced eddy currents and the velocity induced eddy currents, since the laminations are tangent to both the flux and the velocity in the tangential flux thrust bearing.

The magnetic circuit for the radial flux thrust bearing is shown in Fig. 11. It is identical to the fundamental circuit in the tangential flux thrust bearing. The radial bearing has one of these circuits for each annular coil in each stator. The flux in the loop is given by (14) which is identical to (5)

$$\Phi = \frac{NI}{2R_g + R_s + R_r}. \tag{14}$$

The electrically conducting stator section and rotor section will both have a reluctance that increases with frequency because of the eddy currents induced. The effect will be important

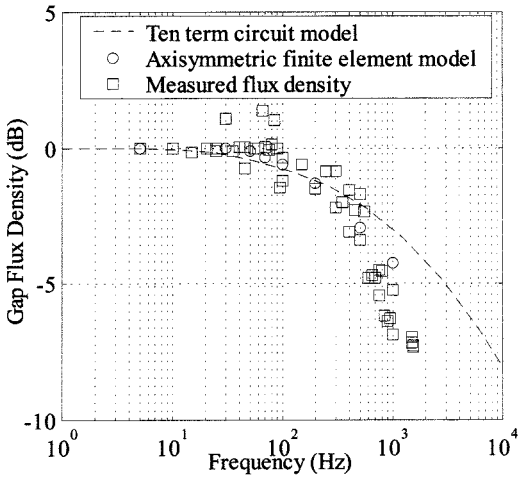

Fig. 12. Measured and predicted gap flux in radial flux thrust bearing.

at a lower frequency in the unlaminated rotor if the stator path is laminated.

Measurements of the flux density in the air gap were made on the bearing for which the finite element model was shown in Fig. 9. The runner inner diameter was 39 mm (1.520 in) and the outer diameter was 66 mm (2.6 in). This radial flux bearing was a little unusual in that the flux path cross section of the outer radius gap was 7.2 times smaller than the cross section of the inner radius gap. Both air gaps were 0.66 mm (0.026 in). The stator and rotor were both unlaminated 430 F stainless steel which has low conductivity, $1.75 \cdot 10^6/\Omega \cdot m$ and relative permeability, 400, to prevent a very low actuator bandwidth. The magnitude of the flux in gap versus frequency as determined by the three methods is shown in Fig. 12. Both the finite element model prediction and the linearized circuit model prediction are close to the experimental measurements for frequencies below the three dB cutoff.

IV. Conclusions

The geometry of tangential flux thrust bearings is such that the flux path is tangential to the laminations of a rotor and stator made from tape wound cores. This is more difficult to accomplish in radial flux thrust bearings. The bandwidth of tangential flux thrust bearings made from tape wound cores is much than it is for solid radial flux thrust bearings.

The frequency dependent circuit method can predict the dynamic response of these bearings. This was shown by comparison of theoretical circuit model results, finite element model results and measurement. Good agreement was found for the laminated tangential flux thrust bearing and the solid radial flux thrust bearing.

Acknowledgment

The authors gratefully acknowledge the support provided for this work from T. Calvert, L. Peterson, and G. Bell of the U.S. Navy NSWC. The tangential flux thrust bearing test rig was designed and built by J. Preuss of the Department of Mechanical Engineering, Texas A&M University.

REFERENCES

[1] I. Toshio, "Magnetic Thrust Bearing," Japanese Patent 59 180 118A2, 1984.

[2] D. W. Lewis and P. E. Allaire, "Control of oscillating transmitted forces in axial-thrust bearings with a secondary magnetic bearing," *ASME Trans.*, vol. 30, no. 1, pp. 1–10, 1987.

[3] R. T. DeWeese, "A Comparison of Eddy Current Effects in a Single Sided Magnetic Thrust Bearing,", Ph.D. dissertation Texas A&M Univ., College Station, 1996.

[4] G. Schweitzer, H. Bleuler, and A. Traxler, *Active Magnetic Bearings*. Zürich, Switzerland: VDF, 1994.

[5] L. Kucera and M. Ahrens, "A model for axial magnetic bearings including eddy currents," in *Proc. 3rd Int. Symp. Magnetic Suspension and Technology*, Tallahassee, FL, 1995, CP-3336, pp. 421–436.

[6] D. C. Meeker, E. C. Maslen, and M. D. Noh, "An augmented circuit model for magnetic bearings including eddy currents, fringing and leakage," *IEEE Trans. Magn.*, vol. 32, pp. 3219–3322, July 1996.

[7] R. L. Stoll, *The Analysis of Eddy Currents*. Oxford, U.K.: Clarendon, 1974.

[8] S. Fukata, Y. Kouya, S. Takashi, M. Yukata, and M. Kugu, "Dynamics of active magnetic thrust bearings," *JSME Int. J.*, ser. III, vol. 34, no. 3, pp. 404–410, 1991.

[9] *Symbolic Math Toolbox Users Guide version 2*, The MathWorks Inc., Natick, MA, 1997.

[10] M. L. Barton, "Loss calculation in laminated steel utilizing anisotropic magnetic permeability," *IEEE Trans. Power App. Syst.*, vol. PAS-99, pp. 1280–1287, May/June 1980.

[11] P. E. Allaire, R. L. Fittro, E. H. Maslen, and W. C. Wakefield, "Eddy currents, magnetic flux and force in solid magnetic thrust bearings," in *Proc. 4th Intl. Symp. Magnetic Bearings*, Zürich, Switzerland, Aug. 1994, pp. 157–163.

Andrew Kenny received the B.S. degree in metallurgical engineering in 1984. He is currently working toward the Ph.D. degree in electromechanical systems at Texas A&M University, College Station.

From 1984 until 1992, he did metallurgical failure analysis on aircraft parts. From 1992 until 2000, he served in the U.S. Air Force where he developed manufacturing and repair processes for aircraft parts.

Alan B. Palazzolo received the Ph.D. degree at the University of Virginia, Charlottesville, in 1981.

Currently, he is a Professor of mechanical engineering at the Texas A&M University, College Station, where he is Director of the Vibration Control and Electromechanics Laboratory. His interests include rotordynamics, active vibration and noise control, magnetic bearings, fluid film bearings, machinery couplings, seal and impeller leakage flow, piping systems, and finite and boundary elements.